Formation of high-field magnetic white dwarfs from common envelopes

Jason Nordhaus[a,1], Sarah Wellons[a], David S. Spiegel[a], Brian D. Metzger[a], and Eric G. Blackman[b]

[a]Department of Astrophysical Sciences, Princeton University, Princeton, NJ 08544; and [b]Department of Physics and Astronomy, University of Rochester, Rochester, NY 14627

Edited by Neta A. Bahcall, Princeton University, Princeton, NJ, and approved January 12, 2011 (received for review October 6, 2010)

The origin of highly magnetized white dwarfs has remained a mystery since their initial discovery. Recent observations indicate that the formation of high-field magnetic white dwarfs is intimately related to strong binary interactions during post-main-sequence phases of stellar evolution. If a low-mass companion, such as a planet, brown dwarf, or low-mass star, is engulfed by a post-main-sequence giant, gravitational torques in the envelope of the giant lead to a reduction of the companion's orbit. Sufficiently low-mass companions in-spiral until they are shredded by the strong gravitational tides near the white dwarf core. Subsequent formation of a super-Eddington accretion disk from the disrupted companion inside a common envelope can dramatically amplify magnetic fields via a dynamo. Here, we show that these disk-generated fields are sufficiently strong to explain the observed range of magnetic field strengths for isolated, high-field magnetic white dwarfs. A higher-mass binary analogue may also contribute to the origin of magnetar fields.

magnetohydrodynamics | compact objects

A significant fraction of isolated white dwarfs form with strong magnetic fields. These high-field magnetic white dwarfs (HFMWDs), the majority of which were discovered via the Sloan Digital Sky Survey [SDSS (1–3)], comprise ∼10% of all isolated white dwarfs (4). Surface field strengths range from a few to slightly less than a thousand megagauss (MG), whereas the bulk of the isolated white dwarf (WD) population have measured weak fields or nondetection upper limits of typically $\lesssim 10^4$–10^5 G (5–7).

In WD-binary systems, the companion's surface is an equipotential. In tight binaries, this equipotential extends toward the WD, leading to mass transfer from the companion onto the WD, a process called "Roche-lobe overflow." Among systems such as these, a possibly even larger fraction of the WD primaries are highly magnetic [i.e., ∼25% of cataclysmic variables; (8)]. Magnetic cataclysmic variables (CVs) are generally divided into two classes: AM Herculis (AM Her) (polars) and DQ Herculis (DQ Her) (intermediate polars). For reviews on AM Her and DQ Her systems, see refs. 9 and 10. Generally, AM Her systems are those in which both components of the binary are synchronously rotating at the orbital period. In this scenario, the formation of an accretion disk is prevented and material is funneled onto the WD via the magnetosphere. Polars have strong magnetic fields ($\sim 10^7$–10^8 G), copious X-ray emission, and stable pulsations in their light curves. On the other hand, DQ Her systems (intermediate polars) are not synchronously locked and have weaker magnetic fields than their polar counterparts, often by an order of magnitude or more. For these systems, an accretion disk forms from which the WD is spun up.

Remarkably, *not a single* observed close, detached binary system (in which the primary is a WD and the companion is a low-mass main-sequence star) contains a HFMWD (11–13). If the magnetic field strengths of white dwarfs were independent of binary interactions, then the observed distribution of isolated WDs should be similar to those in detached binaries. In particular, within 20 pc, there are 109 known WDs (21 of which have a nondegenerate companion), and SDSS has identified 149 HFMWDs (*none* of which has a nondegenerate companion). Assuming binomial statistics, the maximum probability of obtaining samples at least this different from the same underlying population is 5.7×10^{-10}, suggesting at the 6.2-σ level that the two populations are different (for details on this kind of calculation, see Appendix B of ref. 14). Furthermore, SDSS identified 1,253 WD+M-dwarf binaries (*none* of which are magnetic). As was previously pointed out, this suggests that the presence or absence of binarity is crucial in influencing whether a HFMWD results (15). These results initially seem to indicate that HFMWDs preferentially form when isolated. However, unless there is a mechanism by which very distant companions prevent the formation of a strong magnetic field, a more natural explanation is that highly magnetized white dwarfs became that way by engulfing (and removing) their companions.

In the binary scenario, the progenitors of HFMWDs are those systems that undergo a common envelope (CE) phase during post-MS evolution. In particular, magnetic CVs may be the progeny of common envelope systems that almost merge but eject the envelope and produce a close binary. Subsequent orbital reduction via gravitational radiation and tidal forces turn detached systems into those that undergo Roche-lobe overflow. For CEs in which the companion is not massive enough to eject the envelope and leave a tight post-CE binary, the companion is expected to merge with the core. It was suggested that these systems may be the progenitors of isolated HFMWDs (15).

In this paper, we calculate the magnetic fields generated during the common envelope phase. We focus on low-mass companions embedded in the envelope of a post-MS giant. During in-spiral, the companion transfers orbital energy and angular momentum, resulting in differential rotation inside the CE. Coupled with convection, a transient α-Ω dynamo amplifies the magnetic field at the interface between the convective and radiative zones where the strongest shear is available. The fields produced from this interface dynamo are transient and unlikely to reach the white dwarf surface with sufficient strength to explain HFMWD observations. If, however, the companion tidally disrupts, the resultant super-Eddington accretion disk can amplify magnetic fields via a disk dynamo. The disk-generated fields are strong ($\sim 10^1$–10^3 MG), and accretion provides a natural mechanism with which to transport the fields to the WD surface. For a range of disrupted-companion masses, the fields generated in the disk are sufficient to explain the range of observed HFMWDs.

Common Envelope Evolution

Common envelopes are often invoked to explain short period systems in which one component of the binary is a compact star (16–18). The immersion of a companion in a CE with a

Author contributions: J.N. and D.S.S. designed research; J.N., S.W., D.S.S., B.D.M., and E.G.B. performed research; and J.N. wrote the paper.

The authors declare no conflict of interest.

This article is a PNAS Direct Submission.

[1]To whom correspondence should be addressed. E-mail: nordhaus@astro.princeton.edu.

post-main-sequence star can occur via direct engulfment or through orbital decay due to tidal dissipation in the giant's envelope (19–21). Once engulfed, the companion in-spirals due to hydrodynamic drag until it either survives (ejects the envelope leaving a post-CE close binary) or is destroyed. Although CEs can form for various mass-ratio binaries, we focus on low-mass stellar and substellar companions such that the remnant system is expected to be an isolated white dwarf. Because low-mass companions do not release enough orbital energy to eject the envelope, as the orbital separation is reduced, the differential gravitational force due to the proto-WD tidally shreds the companion. The disrupted companion then forms a disk inside the CE that subsequently accretes onto the proto-WD (22). For more detail on the onset and dynamics of the CE phase for post-MS giants and low-mass companions (i.e., low, mass-ratio binaries), see refs. 18 and 19.

Amplification of Magnetic Fields

As a consequence of common envelope evolution, the transfer of orbital energy and angular momentum during in-spiral generates strong shear. Coupled with convection, shear leads to large-scale magnetic field amplification via an α-Ω dynamo. During in-spiral, the free energy in differential rotation available to the dynamo is proportional to the companion mass. In general, the more massive the companion, the more free energy in differential rotation (23). The dynamo converts free energy in differential rotation into magnetic energy, and, therefore, strong shear leads to strong magnetic fields.

Some investigations of the dynamo in this context have imposed a velocity field to determine what steady-state magnetic field might arise if the velocity were steadily driven (24–26). However, as the magnetic field amplifies, differential rotation decreases. In general, for systems in which shear is not resupplied, a transient dynamo and decay of the magnetic field result (27). This scenario was investigated as a way to generate the strong fields necessary to power bipolar outflows in postasymptotic giant branch (post-AGB) and planetary nebulae (PNe) (28, 29). A similar, but weaker, dynamo (akin to the Solar dynamo) may operate in isolated red giant branch and asymptotic giant branch stars (23).

Here, we investigate two scenarios for magnetic field generation during a CE phase between a post-MS giant and a low-mass companion. First, we calculate the magnetic fields at the interface between the convective and radiative zones in the CE (hereafter referred to as the envelope dynamo scenario) and show that this scenario, although potentially viable under special circumstances, is unlikely in general to explain the origin of HFMWDs. As an alternative, we estimate the magnetic fields generated in the disk of a tidally disrupted companion around the proto-WD. The disk-generated fields naturally accrete onto the WD surface and are sufficiently strong to match observations.

Envelope Dynamo The shear profile in a giant star that is produced by a low-mass companion's CE-induced in-spiral leads to a dynamo in the presence of the turbulent convective zone. The field primarily amplifies at $R = R_{\rm conv}$, the interface between the convective and radiative regions. The back-reaction of field amplification on the shear is included with differential rotation and rotation depleting via loss of Poynting flux and turbulent dissipation. For the precise equations solved, generic features of envelope dynamos, and a pictorial representation of the dynamo geometry in isolated stellar and CE settings, see ref. 28. Here we calculate an upper limit to the magnetic field that may be generated by this mechanism, by taking the shear profile in the stellar envelope to be Keplerian (which produces stronger shear than could possibly be maintained in a spherical-hydrostatic star).

Before presenting details of these calculations, we note a few generic features of this type of scenario that might make the envelope dynamo an unlikely explanation of HFMWDs, irrespective of details. There are a few reasons why a field generated at the radiative-convective boundary may not be able to produce strongly magnetized material in the vicinity of the WD. First, as shown below, a robust upper limit to the magnitude of the envelope dynamo generated field is a few times 10^4 G. To explain megagauss fields at the WD surface, this requires an inwardly increasing gradient of **B** (e.g., via field amplification from flux freezing), which might lead the highest-field regions to rise buoyantly, therefore never reaching the WD surface. Second, because the envelope is transient (operates for ~100 years) and the typical AGB lifetime is $\sim 10^5$ years, the envelope would need to be ejected at the time of formation of a HFMWD. Without fine-tuning, this results in a tight, post-CE binary with an undermassive white dwarf—the exact opposite of the observed HFMWDs. Finally, even if the field could penetrate to the WD surface, some mass would need to remain and/or fall back during envelope ejection to anchor the field. A further subtlety is that the transport of magnetic flux into the radiative layer is likely to involve not merely isotropic diffusion but anisotropic diffusion as a downward pumping of magnetic flux involves anisotropic convection. We are led to what seems to be a more natural formation explanation, which is described in the next section. Nevertheless, despite the aforementioned potential difficulties, we now investigate the viability of the envelope dynamo scenario.

Our stellar evolution models were computed using the "Evolve Zero-Age Main Sequence" (EZ) code (30).* We employ a zero-age main-sequence progenitor of 3 $M_\odot$, with solar metallicity at the tip of the AGB. Under the assumption of Keplerian rotation, the saturated toroidal field strength at the base of the 3-$M_\odot$ progenitor's convective zone ($R_{\rm conv} \sim 6 \times 10^{11}$ cm) is roughly $B_\phi \sim 2 \times 10^4$ G. To survive past the PN stage, the fields must reach the WD surface (which is the core of the AGB star, a distance $L \simeq R_{\rm conv}$ interior to the base of the convective zone; see figure 3 of ref. 18 for a pictorial representation), anchor, and sustain or induce a field in the WD. The latter scenario has been investigated by Potter and Tout (31), who conclude that an ordered external field (potentially generated from a dynamo) can induce a surface field on the WD that decays to a few percent of its initial value after a million years.

For the fields to reach the WD surface, radially inward diffusion of magnetic flux must act on a faster time scale than magnetic buoyancy, which transports flux outward. The buoyant-rise velocity, u, is found by equating the upward buoyancy force on a flux tube to the downward viscous drag, thereby obtaining the upward terminal velocity. It may be represented as $u \sim (3Q/8)(a/H_{\rm p})^2(v_a^2/v)$, where $v_a = B/(4\pi\rho)^{1/2}$ is the Alfvén velocity, v is the convective fluid velocity, a is the flux tube radius, $H_{\rm p}$ is a pressure scale height, and Q is a dimensionless quantity of order unity (32). The time to buoyantly rise a distance L from $R_{\rm conv}$, assuming $a \sim L/2$, is $t_{\rm b} = L/u \sim 0.1$ years. The diffusion time scale to traverse a distance L, given a turbulent diffusivity β_ϕ, is $t_{\rm d} = L^2/\beta_\phi$ and must be less than the buoyant-rise time $t_{\rm b}$. This implies a constraint on the turbulent diffusivity: $\beta_\phi > Lu$. For $L \sim 6 \times 10^{11}$ cm, the buoyant-rise velocity of a 2×10^4-G flux tube in an AGB star with $\rho \sim 10^{-4}$ g cm^{-3} requires a diffusivity of at least a few times 10^{17} cm^2 s^{-1}, a very large and physically unlikely value. Note, however, that if weaker fields are generated, the requirement on the diffusivity would lower correspondingly. Furthermore, during one cycle half-period $\tau_{0.5}$ (defined as the time for one reversal of the field), magnetic flux of a given sign (positive or negative) can diffuse into the radiative layer.† After reversal, field of the opposite sign amplifies and diffuses in the

*http://www.astro.wisc.edu/~townsend/static.php?ref=ez-web.

†Though the cycle period does increase in the dynamical regime, it does not deviate significantly from the half-cycle kinematic value we use here [$\tau \sim 0.03$ y); (28)]. Note that although the radiative layer is convectively stable, it may still possess nonnegligible turbulence.

radiative layer. Therefore, the diffusion time scale must not be greater than the cycle half-period: $t_d \leq \tau_{0.5}$. This implies another theoretical constraint on the turbulent diffusivity for consistency of our dynamo model, namely $\beta_\phi \geq L^2/\tau_{0.5}$. This latter constraint yields $\beta_\phi \gtrsim 4 \times 10^{17}$ cm^2 s^{-1}. A subtlety is that the transport would not be a strictly isotropic diffusion but could be the result of down pumping by anisotropic convection (33).

One way to infer the turbulent diffusivity in evolved stars is to note that isotopic anomalies in low-mass red giant branch and AGB stars require that material from the base of the convective zone be transported to near the H-burning shell, processed, and returned to the convective envelope (34, 35). This so-called "cool bottom processing" (CBP) is thought to be magnetically driven (23, 36). In the magnetic mixing scenario, a lower bound on the turbulent diffusivity is $\sim 7 \times 10^{15}$ cm^2 s^{-1} (23). Although the actual diffusion coefficients in evolved star interiors are unknown, the values inferred from CBP are more than an order of magnitude lower than what are required for the envelope dynamo scenario to transport $\sim 10^4$-G fields all the way to the WD surface. Higher field strengths (in particular, ~MG fields) lead to shorter buoyant-rise times and smaller cycle half-periods and, therefore, require even greater diffusivity. In short, a substantial macroscopic diffusivity would be needed to transport megagauss fields to the WD surface in AGB stars. We presently do not have independent constraints on these coefficients.

Disk Dynamo. If the field generated in the envelope cannot diffuse to the WD surface, an alternative possibility is amplification in an accretion disk that forms when the companion is tidally disrupted inside the common envelope (22). As shown below, this scenario is attractive because it provides a natural mechanism for transporting the field to the proto-WD surface.

We consider disks formed from companions spanning the range from sub-Jupiter-mass planets (see below) to brown dwarfs to low-mass stars (i.e., M_c between $\sim 0.1 M_J$ and a few times $10^2 M_J$).[‡] Tidal disruption of the companion results in formation of a disk inside the AGB star. This occurs at the tidal shredding radius, which we estimate as $R_s \simeq R_c (2M/M_c)^{1/3}$, where r_c and M_c are the radius and mass of the companion and M is the stellar mass interior to R_s (19). We note that, because planetary and low-mass stellar companions to solar-type stars are significantly more plentiful than brown dwarfs (38–40), disks at the upper or lower mass range may be more common than those in the intermediate mass range.

The disk is ionized and susceptible to the development of magnetized turbulence [e.g., via the magnetorotational instability (41)]. Accretion toward the central proto-WD occurs on a viscous time scale given by $t_{visc} \simeq R^2/\nu \simeq P_{orb}/\alpha_{ss}(H/R)^2$, where P_{orb} is the Keplerian orbital period at radius R, $\nu = \alpha_{ss} c_s H = \alpha_{ss}(H/R)^2 R^2 \Omega$ is the effective kinematic viscosity, H is the disk scale height, $c_s = H\Omega$ is the midplane sound speed, $\Omega = 2\pi/P_{orb}$ is the Keplerian orbital frequency, and α_{ss} is the dimensionless Shakura–Sunyaev parameter that characterizes the efficiency of angular momentum transport (42). The initial accretion rate can be approximated as

$$\dot{M} \sim \frac{M_c}{t_{visc}|_{r_s}} \approx 7 M_\odot \text{ y}^{-1} \times \left(\frac{\alpha_{ss}}{10^{-2}}\right)\left(\frac{M_c}{30 M_J}\right)^{3/2}\left(\frac{r_c}{r_J}\right)^{-1/2}\left(\frac{H/R}{0.5}\right)^2, \quad [1]$$

where we have scaled r_c to the radius of Jupiter[§] and have scaled H/R to a large value ~0.5 because the disk cannot cool efficiently at such high accretion rates and would be geometrically thick. Because the companions under consideration lead to disks much more dense than the stellar envelope, it is reasonable to ignore any interaction between the disk and the star.

Formula **1** illustrates that for $M_c \sim 0.1$–$500 M_J$, and for typical values of $\alpha_{ss} \sim 0.01$–0.1, $\dot{M}$ is ~3 to 9 orders of magnitude larger than the Eddington accretion rate of the proto-WD (i.e., $\dot{M}_{Edd} \sim 10^{-5} M_\odot$ y^{-1}). At first, it might seem apparent that inflow of mass onto the WD surface would be inhibited by radiation pressure in such a scenario. However, this neglects the fact that, at sufficiently high accretion rates, photons are trapped and advected to small radii faster than they can diffuse out (43–47). In this "hypercritical" regime, accretion is possible even when $\dot{M} \gg \dot{M}_{Edd}$.

We evaluate the possibility of hypercritical accretion by estimating the radius interior to which the inward accretion time scale, t_{visc} is less than the time scale for photons to diffuse out of the disk midplane, t_{diff} [which is approximately $H\tau/c$, where τ is the vertical optical depth (44, 45, 48)]. This "trapping radius" (tr) is given by $R_{tr} = \dot{M}\kappa H/4\pi R c$, where κ is the opacity. An important quantity is the ratio of the trapping radius to the outer disk radius R_s (coincident with the tidal shredding radius):

$$\frac{R_{tr}}{R_s} \approx 1.0 \times 10^4 \left(\frac{\alpha_{ss}}{10^{-2}}\right)\left(\frac{\kappa}{\kappa_{es}}\right) \times \left(\frac{M_c}{30 M_J}\right)^{11/6}\left(\frac{M_{WD}}{0.6 M_\odot}\right)^{-1/3}\left(\frac{r_c}{r_J}\right)^{-3/2}\left(\frac{H/R}{0.5}\right)^3, \quad [2]$$

where we have used formula **1** and scaled κ to the electron scattering opacity $\kappa_{es} = 0.4$ cm^2 g^{-1}. If $R_s < R_{tr}$, then $t_{visc} < t_{diff}$ and photons are advected with the matter.

From formula **2** we conclude that $R_{tr} > R_s$ for $M_c \gtrsim 0.1 M_J$. This implies that photon pressure will be unable to halt accretion initially and that the local energy released by accretion must be removed by advection (49). Advection acts like a conveyor belt, nominally carrying the gas to small radii as its angular momentum is removed. If, however, there is no sink for the hot gas, this conveyor may "jam.". This is an important distinction between white dwarfs and neutron stars or black holes, as the latter two can remove the thermal energy by neutrino cooling or advection through the event horizon, respectively. In contrast to a WD, neutrino cooling is ineffective and thermal pressure builds, such that radiation pressure may again become dynamically significant (47). This in turn shuts down the accretion to at most, the Eddington rate.

However, this scenario neglects the possibility of outflows[¶], which can sustain inflow by carrying away the majority of the thermal energy, thereby allowing a smaller fraction of the material to accrete at a higher than Eddington rate. Though more work is needed to assess the efficiency of outflows in the present context, radiatively inefficient accretion flows are widely thought to be prone to powerful outflows (49–54). Even if accretion occurs at, or near, the Eddington rate, the fields produced ($\gtrsim$10 MG) are still strong enough to explain the bulk of the magnetized WD population. The origin of the strongest field systems (~100–1,000 MG) may be problematic if accretion is limited to the Eddington rate.

Nevertheless, the material deposited outside the WD will be hot and virialized, forming an extended envelope with a length scale comparable to the radius. Though initially hot, this material will eventually cool (on longer, stellar time scales) and become incorporated into the stellar layers near the proto-WD surface. If this material cools at some fraction of the local Eddington

[‡] M_J is the mass of Jupiter. This classification as planet or brown dwarf is based solely on mass (37).

[§] r_J is the radius of Jupiter. Note that r_c depends only weakly on mass for the companions we consider.

[¶] It is interesting to note that the presence of such outflows in the present context is coincident with the prevalence of bipolar protoplanetary nebulae.

luminosity, it will be incorporated onto the WD surface on a time scale $\sim 10^2$–10^4 y, which is much less than typical AGB lifetimes.

A final complication may arise because the composition of the companion is likely to be hydrogen-rich and will begin to burn thermonuclearly as material accretes or after it settles on the proto-WD surface. Because the energy released in burning hydrogen to helium ($\sim$7 MeV nucleon^{-1}) vastly exceeds the gravitational binding energy per nucleon at the WD surface ($\sim$0.1 MeV nucleon^{-1}), burning that occurs explosively could have a dynamical impact. For the accretion rates of relevance, we estimate that the midplane temperature of the disk exceeds $\sim 10^8$ K, such that hydrogen will burn via the hot CNO cycle. The hot CNO cycle occurs at a rate that is independent of temperature and is itself thermally stable. However, hydrogen-rich material deposited in the He burning layer may, under some circumstances, trigger a thermonuclear runaway (55), which could remove the accreted mass from the proto-WD surface, or even eject the common envelope entirely. In what follows we assume stable burning and set aside this important caveat. Additional work will, however, be required to address what conditions are required for stable versus explosive burning.

Because of the presence of shear in the disk,[‖] the MRI is a likely source of turbulence, which in turn amplifies magnetic field. Large-scale fields produced by the MRI have been modeled via α-Ω dynamos at various levels of sophistication (see ref. 57 for the most recent example). However, for the purposes of estimating orders of magnitude of the fields, approximate values from less sophisticated treatments can be employed. Although this situation is qualitatively similar to that described in the previous subsection, the dynamo we envision here operates in the accretion disk and not the envelope. The Alfvén velocity in the disk obeys $v_a^2 = \alpha_{ss} c_s^2$ (58), such that the mean toroidal field at radius R is given by (58)

$$\overline{B}_\phi \sim \left(\frac{\dot{M}\Omega}{R}\frac{R}{H}\right)^{1/2} \approx 160\ \mathrm{MG}\left(\frac{\eta_{acc}}{0.1}\right)^{1/2}\left(\frac{\alpha_{ss}}{10^{-2}}\right)^{1/2}\left(\frac{M_c}{30M_J}\right)^{3/4}\times \left(\frac{M_{WD}}{0.6M_\odot}\right)^{1/4}\left(\frac{r_c}{r_J}\right)^{-1/4}\left(\frac{H/R}{0.5}\right)^{1/2}\left(\frac{R}{10^9\ \mathrm{cm}}\right)^{-3/4}, \quad [3]$$

where in the second equality we have substituted formula **1** for $\dot{M}$ and multiplied by the factor $0.1 \lesssim \eta_{acc} \leq 1$ to account for the possibility of outflows as described above. If an α-Ω dynamo operates, the mean poloidal field $\overline{B}_p$ is related to the toroidal field via $\overline{B}_p = \alpha_{ss}^{1/2}\overline{B}_\phi$ (58). However, regardless of whether a large-scale field is generated, a turbulent field of magnitude $\overline{B}_\phi$ is likely to be present and contributing significantly to the Maxwell stresses responsible for disk accretion.

Fig. 1 shows the toroidal field evaluated near the WD surface $R \approx R_{WD} \approx 10^9$ cm as a function of companion mass M_c, calculated for two different values of the viscosity ($\alpha_{ss} = 0.01$ and 0.1). In both cases, we assume that $\eta_{acc} = 0.1$. Note that for the range of relevant companion masses $M_c \sim 0.1$–$500\ M_J$, $\overline{B}_\phi \sim 10$–1,000 MG, in precisely the correct range to explain the inferred surface field strengths of HFMWDs.

Although our results suggest that companion accretion can produce the field strengths necessary to explain HFMWDs, for the field to be present on the surface of the WD when it forms, it must at a minimum survive the remaining lifetime of the star. In particular, the field will decay due to ohmic diffusion on the time scale

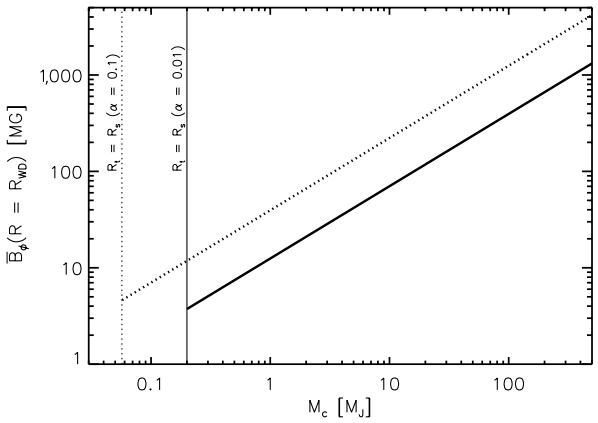

Fig. 1. Toroidal magnetic field strength, $\overline{B}_\phi$ formula **3**, at the WD surface as a function of the mass of the tidally disrupted companion M_c. Toroidal field strengths are presented for two values of the viscosity, $\alpha_{ss} = 0.01$ (solid line) and $\alpha_{ss} = 0.1$ (dotted line) and assuming an accretion efficiency $\eta_{acc} = 0.1$. The white dwarf mass and radius are $M_{WD} = 0.6\ M_\odot$ and $r_{WD} = 10^9$ cm, respectively. The vertical lines show the companion mass above which photons are trapped in the accretion flow (i.e., $r_{tr} > r_s$; formula **2**), such that super-Eddington accretion occurs.

$$\tau_{decay} \sim \frac{3(\Delta R)^2}{\eta_s} \sim 4\times 10^6\ \mathrm{y}\left(\frac{T}{10^8\ \mathrm{K}}\right)^{3/2}\times \left(\frac{\ln\Lambda}{10}\right)^{-1}\left(\frac{R_{WD}}{10^9\ \mathrm{cm}}\right)^2\left(\frac{M_{WD}}{0.6M_\odot}\right)^{-2}\left(\frac{\eta_{acc}}{0.1}\right)^2\left(\frac{M_c}{30M_J}\right)^2, \quad [4]$$

where $\eta_s \approx 5\times 10^{12}(\ln\Lambda/10)T^{3/2}$ cm^2 s^{-1} is the Spitzer resistivity, $\ln\Lambda$ is the Coulomb logarithm, T is the stellar temperature near the proto-WD surface, and $\Delta R = \eta_{acc}M_c/4\pi r_{WD}^2\bar{\rho}$ is the final thickness of the accreted companion mass after it is incorporated into the surface layers of proto-WD, where $\bar{\rho} \equiv M_{WD}/(4\pi r_{WD}^3/3)$ is the mean density of the proto-WD.

Formula **4** shows that for typical core temperatures during the AGB phase $T \sim 10^8$ K, τ_{decay} exceeds the mean AGB lifetime $\tau_{AGB} \sim$ Myr for $M_c \gtrsim 20M_J$. This suggests that fields may survive ohmic decay, at least for very massive companions. Furthermore, the magnetized companion material may become incorporated into the degenerate WD core long before the AGB phase ends, in which case the much higher conductivity due to degenerate electrons substantially increase the ohmic decay time scale over that given by formula **4**, thereby ensuring long-term field survival.

Conclusions

Recent observational evidence from the Sloan Digital Sky Survey strongly suggests that high-field magnetic white dwarfs originate from binary interactions. In particular, it was proposed that the progenitors of HFMWDs are binary systems that evolve through a common envelope phase (15). In this scenario, companions that survive CE evolution (leaving tight binaries) may produce magnetic cataclysmic variables, whereas those that do not survive (i.e., that merge) may produce isolated HFMWDs.

To investigate this hypothesis, we have estimated the magnetic fields resulting from a low-mass companion embedded in a CE phase with a post-MS giant. During in-spiral, the companion transfers energy and angular momentum to the envelope. The resulting shearing profile, coupled with the presence of convection, can amplify large-scale magnetic fields via dynamo action in the envelope. We incorporate the back-reaction of the magnetic field growth on the shear, which results in a transient dynamo. The fields generated at the interface between the convective and radiative zones are weak ($\sim 2\times 10^4$ G) and would have to diffuse to the WD surface and anchor there if they are to explain the HFMWDs. A successful envelope dynamo scenario must also

[‖]For black hole disks, differential rotation near the disk midplane is preserved even in a thick-disk, super-Eddington context (56). However, for white dwarf disks, photons are not advected into, and lost to, the black hole.

survive to the end of the AGB phase, which probably means only if the companion ejects the turbulent envelope; the dynamo is transient as long as there is a source of turbulent diffusion. The bulk of the systems formed this way might be post-CE, tight binaries—potentially magnetic CVs.

To explain isolated HFMWDs, an alternative to a dynamo operating in the envelope is a dynamo operating in an accretion disk. During the CE phase, if the companion is of sufficiently low mass, it avoids prematurely ejecting the envelope. Instead, inspiral proceeds until the companion is tidally shredded by the gravitational field of the proto-WD. The subsequent formation of an accretion disk, which also possesses turbulence and shear, can amplify magnetic fields via dynamo action. For the range of disrupted companions considered here, the disk initially accretes at super-Eddington values. In this hypercritical regime, the time scale for photon diffusion out of the disk is longer than the viscous time scale. For a range of disrupted-companion disks, we find that the saturated toroidal mean field attains values between a few and a few thousand megagauss. Amplification of the magnetic field in a super-Eddington accretion disk is attractive as it reproduces the observed range of HFMWDs and naturally transports magnetic flux to the WD surface.

High-mass stars may also undergo common envelope interactions in the presence of close companions. If the common envelope field mechanisms described here operate in high-mass stars, then the result could be strong field neutron stars or magnetars (neutron stars with magnetic fields in excess of $\sim 10^{14}$–10^{15} G). In particular, formation of an accretion disk from an engulfed companion during a red supergiant phase could produce a magnetized WD core. In the eventual core collapse and stellar supernova explosion [possibly driven by the neutrino mechanism; (59)], the magnetized WD core collapses to a neutron star. If simple flux freezing operates (itself an open question) and the initial magnetized core is on the order of ~100–1,000 MG, homologous collapse to a neutron star would generate $\sim 10^{14}$–10^{15} G fields. Typical neutron stars that possess modest field strengths may originate from core-collapse supernova of single stars or stars without having incurred a CE phase. Note that what we are proposing here is an alternative to the neutrino-driven convection dynamo described in refs. 60 and 61. In our model, the engulfment of a companion and the formation of an accretion disk naturally provides fast rotation, magnetized turbulence, and differential rotation. We emphasize that the viability of this mechanism depends on the length scale of the magnetic field deposited in the precollapse core, which must be sufficiently large to produce, upon collapse, the dipole-scale, volume-encompassing fields necessary to account for the spin-down behavior of magnetars and the energy budget of their giant flares (62).

In summary, common envelope evolution as the origin of strongly magnetized, compact objects seems plausible. Whether this hypothesis is ultimately found to be viable will depend on the statistics of low-mass stellar and substellar companions to stars of similar masses to (or somewhat higher masses than) the Sun. The numerous radial velocity searches of the last 20 y have revealed a number of such companions (63–65). The precise occurrence rate of companions in orbits that could lead to the kind of disk-dynamo mechanism described above remains unclear (though if such companions turn out to be rarer than the HFMWD fraction, then the SDSS data indicating a binary origin would be puzzling). Further theoretical work into the binary origin of HFMWDs and magnetars requires the development of multidimensional, magnetohydrodynamic simulations of the CE phase. Such an approach has already had initial success for purely hydrodynamic adaptive mesh refinement simulations (66).

ACKNOWLEDGMENTS. We thank Alberto Lopez, Jay Farihi, Jim Stone, Jeremy Goodman, Kristen Menou, Deepak Raghavan, Andrei Mesinger, Adam Burrows, and Fergal Mullally for thoughtful discussions. J.N. acknowledges support for this work from NASA Grant HST-AR-12146. D.S.S. acknowledges support from National Aeronautics and Space Administration (NASA) Grant NNX07AG80G. Support for B.D.M. is provided by NASA through Einstein Postdoctoral Fellowship Grant PF9-00065 awarded by the Chandra X-Ray Center, which is operated by the Smithsonian Astrophysical Observatory for NASA under Contract NAS8-03060. E.G.B. acknowledges support from National Science Foundation Grants PHY-0903797 and AST-0807363.

1. Gänsicke BT, Euchner F, Jordan S (2002) Magnetic white dwarfs in the Early Data Release of the Sloan Digital Sky Survey. *Astron Astrophys* 394:957–963.
2. Schmidt GD, et al. (2003) Magnetic white dwarfs from the Sloan Digital Sky Survey: The first data release. *Astrophys J* 595:1101–1113.
3. Vanlandingham KM, et al. (2005) Magnetic white dwarfs from the SDSS. II. The second and third data releases. *Astron J* 130:734–741.
4. Liebert J, Bergeron P, Holberg JB (2003) The true incidence of magnetism among field white dwarfs. *Astron J* 125:348–353.
5. Kawka A, Vennes S, Schmidt GD, Wickramasinghe DT, Koch R (2007) Spectropolarimetric survey of hydrogen-rich white dwarf stars. *Astrophys J* 654:499–520.
6. Valyavin G, et al. (2006) A search for kilogauss magnetic fields in white dwarfs and hot subdwarf stars. *Astrophys J* 648:559–564.
7. Aznar Cuadrado R, et al. (2004) Discovery of kilogauss magnetic fields in three DA white dwarfs. *Astron Astrophys* 423:1081–1094.
8. Wickramasinghe DT, Ferrario L (2000) Magnetism in isolated and binary white dwarfs. *Publ Astron Soc Pac* 112:873–924.
9. Patterson J (1994) The DQ Herculis stars. *Publ Astron Soc Pac* 106:209–238.
10. Wickramasinghe DT, Ferrario L (2000) Accretion and magnetic field structure in AM Herculis systems. *New Astron Rev* 44:69–74.
11. Liebert J, et al. (2005) Where are the magnetic white dwarfs with detached, nondegenerate companions? *Astron J* 129:2376–2381.
12. Silvestri NM, et al. (2006) A catalog of spectroscopically selected close binary systems from the Sloan Digital Sky Survey data release four. *Astron J* 131:1674–1686.
13. Silvestri NM, et al. (2007) New close binary systems from the SDSS-I (data release five) and the search for magnetic white dwarfs in cataclysmic variable progenitor systems. *Astron J* 134:741–748.
14. Spiegel DS, Paerels F, Scharf CA (2007) A possible dearth of hot gas in galaxy groups at intermediate redshift. *Astrophys J* 658:288–298.
15. Tout CA, Wickramasinghe DT, Liebert J, Ferrario L, Pringle JE (2008) Binary star origin of high field magnetic white dwarfs. *Mon Not R Astron Soc* 387:897–901.
16. Paczynski B (1976) Common Envelope Binaries. *Structure and Evolution of Close Binary Systems*, International Astronomical Union Symposium, eds P Eggleton, S Mitton, and J Whelan p:75.
17. Iben I, Jr, Livio M (1993) Common envelopes in binary star evolution. *Publ Astron Soc Pac* 105:1373–1406.
18. Nordhaus J, Blackman EG (2006) Low-mass binary-induced outflows from asymptotic giant branch stars. *Mon Not R Astron Soc* 370:2006–2012.
19. Nordhaus J, Spiegel DS, Ibgui L, Goodman J, Burrows A (2010) Tides and tidal engulfment in post-main-sequence binaries: Period gaps for planets and brown dwarfs around white dwarfs. *Mon Not R Astron Soc* 408:631–641.
20. Carlberg JK, Majewski SR, Arras P (2009) The role of planet accretion in creating the next generation of red giant rapid rotators. *Astrophys J* 700:832–843.
21. Villaver E, Livio M (2009) The orbital evolution of gas giant planets around giant stars. *Astrophys J Lett* 705:L81–L85.
22. Reyes-Ruiz M, López JA (1999) Accretion disks in pre-planetary nebulae. *Astrophys J* 524:952–960.
23. Nordhaus J, Busso M, Wasserburg GJ, Blackman EG, Palmerini S (2008) Magnetic mixing in red giant and asymptotic giant branch stars. *Astrophys J Lett* 684:L29–L32.
24. Tout CA, Pringle JE (1992) Spin-down of rapidly rotating, convective stars. *Mon Not R Astron Soc* 256:269–276.
25. Regos E, Tout CA (1995) The effect of magnetic fields in common-envelope evolution on the formation of cataclysmic variables. *Mon Not R Astron Soc* 273:146–156.
26. Blackman EG, Frank A, Markiel JA, Thomas JH, Van Horn HM (2001) Dynamos in asymptotic-giant-branch stars as the origin of magnetic fields shaping planetary nebulae. *Nature* 409:485–487.
27. Blackman EG, Nordhaus JT, Thomas JH (2006) Extracting rotational energy in supernova progenitors: Transient Poynting flux growth vs. turbulent dissipation. *New Astron* 11:452–464.
28. Nordhaus J, Blackman EG, Frank A (2007) Isolated versus common envelope dynamos in planetary nebula progenitors. *Mon Not R Astron Soc* 376:599–608.
29. Nordhaus J, et al. (2008) Towards a spectral technique for determining material geometry around evolved stars: Application to HD 179821. *Mon Not R Astron Soc* 388:716–722.
30. Paxton B (2004) EZ to evolve ZAMS stars: A program derived from Eggleton's Stellar Evolution Code. *Publ Astron Soc Pac* 116:699–701.
31. Potter AT, Tout CA (2010) Magnetic field evolution of white dwarfs in strongly interacting binary star systems. *Mon Not R Astron Soc* 402:1072–1080.
32. Parker EN (1979) *Cosmical Magnetic Fields: Their Origin and Their Activity* (Oxford Univ Press, New York).
33. Tobias SM, Brummell NH, Clune TL, Toomre J (1998) Pumping of magnetic fields by turbulent penetrative convection. *Astrophys J Lett* 502:L177–L180.
34. Wasserburg GJ, Boothroyd AI, Sackmann I.-J (1995) Deep circulation in red giant stars: A solution to the carbon and oxygen isotope puzzles? *Astrophys J Lett* 447:L37–L40.

35. Nollett KM, Busso M, Wasserburg GJ (2003) Cool bottom processes on the thermally pulsing asymptotic giant branch and the isotopic composition of circumstellar dust grains. *Astrophys J* 582:1036–1058.
36. Busso M, Wasserburg GJ, Nollett KM, Calandra A (2007) Can extra mixing in RGB and AGB stars be attributed to magnetic mechanisms? *Astrophys J* 671:802–810.
37. Spiegel DS, Burrows A, Milsom JA (2011) The deuterium-burning mass limit for brown dwarfs and giant planets. *Astrophys J* 727:57.
38. Wright JT, et al. (2009) Ten new and updated multiplanet systems and a survey of exoplanetary systems. *Astrophys J* 693:1084–1099.
39. Marcy GW, Butler RP (2000) Planets orbiting other suns. *Publ Astron Soc Pac* 112:137–140.
40. Farihi J, Becklin EE, Zuckerman B (2005) Low-luminosity companions to white dwarfs. *Astrophys J Suppl* 161:394–428.
41. Balbus SA, Hawley JF (1998) Instability, turbulence, and enhanced transport in accretion disks. *Rev Mod Phys* 70:1–53.
42. Shakura NI, Sunyaev RA (1973) Black holes in binary systems. Observational appearance. *Astron Astrophys* 24:337–355.
43. Colgate SA (1971) Neutron-star formation, thermonuclear supernovae, and heavy-element reimplosion. *Astrophys J* 163:221–230.
44. Katz JI (1977) X-rays from spherical accretion onto degenerate dwarfs. *Astrophys J* 215:265–275.
45. Blondin JM (1986) Hypercritical spherical accretion onto compact objects. *Astrophys J* 308:755–764.
46. Chevalier RA (1989) Neutron star accretion in a supernova. *Astrophys J* 346:847–859.
47. Houck JC, Chevalier RA (1992) Linear stability analysis of spherical accretion flows onto compact objects. *Astrophys J* 395:592–603.
48. Begelman MC (1979) Can a spherically accreting black hole radiate very near the Eddington limit. *Mon Not R Astron Soc* 187:237–251.
49. Spruit HC (2001) Radiatively inefficient accretion discs. *The Neutron Star–Black Hole Connection, Proceedings of the NATO Advanced Study Institute, ELOUNDA, 1999*, NATO Science Series C: Mathematical and Physical Sciences, eds C Kouveliotou, J Ventura, and E van den Heuvel (Kluwer Academic Publishers, Dordrecht, The Netherlands), Vol 567.
50. Narayan R, Yi I (1995) Advection-dominated accretion: Underfed black holes and neutron stars. *Astrophys J* 452:710–735.
51. Blandford RD, Begelman MC (1999) On the fate of gas accreting at a low rate on to a black hole. *Mon Not R Astron Soc* 303:L1–L5.
52. Armitage PJ, Livio M (2000) Black hole formation via hypercritical accretion during common-envelope evolution. *Astrophys J* 532:540–547.
53. Hawley JF, Balbus SA (2002) The dynamical structure of nonradiative black hole accretion flows. *Astrophys J* 573:738–748.
54. Ohsuga K, Mori M, Nakamoto T, Mineshige S (2005) Supercritical accretion flows around black holes: Two-dimensional, radiation pressure-dominated disks with photon trapping. *Astrophys J* 628:368–381.
55. Podsiadlowski P, Ivanova N, Justham S, Rappaport S (2010) Explosive common-envelope ejection: Implications for gamma-ray bursts and low-mass black-hole binaries. *Mon Not R Astron Soc* 406:840–847.
56. Qian L, et al. (2009) The Polish doughnuts revisited. I. The angular momentum distribution and equipressure surfaces. *Astron Astrophys* 498:471–477.
57. Gressel O (2010) A mean-field approach to the propagation of field patterns in stratified magnetorotational turbulence. *Mon Not R Astron Soc* 405:41–48.
58. Blackman EG, Frank A, Welch C (2001) Magnetohydrodynamic stellar and disk winds: Application to planetary nebulae. *Astrophys J* 546:288–298.
59. Nordhaus J, Burrows A, Almgren A, Bell J (2010) Dimension as a key to the neutrino mechanism of core-collapse supernova explosions. *Astrophys J* 720:694–703.
60. Duncan RC, Thompson C (1992) Formation of very strongly magnetized neutron stars —Implications for gamma-ray bursts. *Astrophys J Lett* 392:L9–L13.
61. Thompson C, Duncan RC (1993) Neutron star dynamos and the origins of pulsar magnetism. *Astrophys J* 408:194–217.
62. Woods PM, Thompson C (2006) Soft gamma repeaters and anomalous X-ray pulsars: Magnetar candidates. *Compact Stellar X-Ray Sources*, Cambridge Astrophysics Series, eds W Lewin and M van der Klis (Cambridge University Press, Cambridge, UK), Vol 39, pp 547–586.
63. Duquennoy A, Mayor M (1991) Multiplicity among solar-type stars in the solar neighbourhood. II—Distribution of the orbital elements in an unbiased sample. *Astron Astrophys* 248:485–524.
64. Halbwachs JL, Mayor M, Udry S, Arenou F (2003) Multiplicity among solar-type stars. III. Statistical properties of the F7-K binaries with periods up to 10 years. *Astron Astrophys* 397:159–175.
65. Raghavan D, et al. (2010) A survey of stellar families: Multiplicity of solar-type stars. *Astrophys J Suppl* 190:1–42.
66. Ricker PM, Taam RE (2008) The interaction of stellar objects within a common envelope. *Astrophys J Lett* 672:L41–L44.